Two-photon decay of the $2\,^1S_0$ state in He-like bromine

R. W. Dunford, H. G. Berry, S. Cheng, E. P. Kanter, C. Kurtz, and B. J. Zabransky
Physics Division, Argonne National Laboratory, Argonne, Illinois 60439

A. E. Livingston
Department of Physics, University of Notre Dame, Notre Dame, Indiana 46556

L. J. Curtis
Department of Physics and Astronomy, University of Toledo, Toledo, Ohio 43606
(Received 26 October 1992)

We report a measurement of the lifetime of the $1s2s\ ^1S_0$ state in two-electron Br^{33+}. This state decays to the $1s^2\ ^1S_0$ ground state only by the simultaneous emission of two photons. Ions in the $1s2s\ ^1S_0$ level are produced by excitation of energetic bromine ions in a thin carbon foil. The lifetime is determined by measuring the change in the rate of two-photon coincidences as a function of the foil-detector separation. The lifetime measurement yields 39.32(32) ps in agreement with a theoretical value of 39.63(16) ps.

PACS number(s): 32.70.Fw, 31.30.Jv, 31.10.+z

I. INTRODUCTION

The history of two-photon decay began with the work of Goeppert-Mayer [1,2] who suggested that the dominant decay mode for the $2\,^2S_{1/2}$ state in hydrogen was the simultaneous emission of two photons. This conclusion was confirmed by Breit and Teller [3] who studied the decay of the $2s$ states of hydrogen and helium. For hydrogen, they estimated that the two-photon decay rate for the $2\,^2S_{1/2}$ state is about $7\ s^{-1}$, while the magnetic dipole ($M1$) decay rate is about $5\times10^{-6}\ s^{-1}$. For helium, the single-photon decay of the $2\,^1S_0$ state is strictly forbidden by angular-momentum considerations because the initial and final states have zero angular momentum while the emitted photon has spin one. Breit and Teller estimated that the decay rate for the $2\,^1S_0$ state of helium would be of the same order of magnitude as that of the $2\,^2S_{1/2}$ state of hydrogen.

Two-photon decay [4] proceeds via electric-dipole couplings to virtual excited states, which requires that the photons be emitted simultaneously. For the He-like $2\,^1S_0$ state and the H-like $2\,^2S_{1/2}$ state, the energies of the individual photons have a continuous distribution with a peak at half the transition energy dropping to zero at either end point. For each decay, the sum of the energies (E_1, E_2) of the two photons is equal to the transition energy E_0

$$E_0=E_1+E_2\ , \tag{1}$$

and they are emitted with an angular correlation $(1+\cos^2\theta)$.

Accurate nonrelativistic calculations for hydrogen and one-electron ions have been made by Spitzer and Greenstein [5], Shapiro and Breit [6], Zon and Rapoport [7], Klarsfeld [8,9] and Drake [10]. Drake's result is

$$\omega_{\rm nr}(2\,^2S_{1/2}\ 2E1)=8.229\,38Z^6\ s^{-1}\ , \tag{2}$$

showing the characteristic Z^6 dependence on the nuclear charge Z. Fully relativistic calculations of the H-like decay rate have been done by Parpia and Johnson [11,12] and by Goldman and Drake [13,14].

Dalgarno [15,16] made the first calculation of the two-photon decay of the $2\,^1S_0$ state of helium; performing an explicit summation over intermediate discrete and continuum states. Other calculations for helium and light He-like ions have been made by Victor [17,18], Jacobs [19], and Drake, Victor, and Dalgarno [20]. More recently, Drake [10] calculated the nonrelativistic decay rates for all two-electron ions up to $Z=92$. In his calculation, the infinite summation over discrete and continuum states was replaced by a finite summation over discrete states. His nonrelativistic result is expressed by the formula

$$\bar{\omega}_{\rm nr}=16.458\,762(Z-0.806\,389)^6\times\left[1+\frac{1.539}{(Z+2.5)^2}\right]\ s^{-1}\ . \tag{3}$$

For bromine ($Z=35$) this gives a lifetime

$$\tau_{\rm nr}=37.971\,52\ {\rm ps}\ . \tag{4}$$

Detailed calculations of relativistic corrections to the decay rate of the $2\,^1S_0$ state have not been done, but Drake [10] has estimated these effects by applying screening corrections to the relativistic decay rate for one-electron ions. His result for bromine is

$$\tau_{\rm rel}=39.63(16)\ {\rm ps}\ . \tag{5}$$

Comparing Eqs. (4) and (5), the relativistic corrections are about 4%.

A pioneering observation of two-photon decay was made by Lipeles, Novick, and Tolk [21,22] in He^+. They observed two-photon coincidences and verified the $(1+\cos^2\theta)$ dependence for the opening angle between the

two photons. Measurements of the lifetime of the $2\,^2S_{1/2}$ level have been made in He^+ [22–24], O^{7+} [25], F^{8+} [25], S^{15+} [26], Ar^{17+} [26], and Ni^{27+} [27]. The two-photon decay mode in He-like ions was established by Marrus and Schmieder [26] by observing coincidences in Ar^{16+}. The lifetime of the $2\,^1S_0$ level has been measured to about 1% in Kr^{34+} [28] and Ni^{26+} [27] and to lower precision in helium [29,30], Li^+ [31], and Ar^{16+} [26].

The main motivation for further measurements of the lifetimes of two-photon emitting states is to provide more information on the relativistic corrections to the decay rate. Such measurements can best be done using high-Z ions since the relativistic effects are larger. The He-like ions are more interesting theoretically since both relativistic corrections and two-electron correlations are important. The problem of understanding the structure of these ions has motivated recent theoretical and experimental studies of transition energies [32,33]. Lifetime measurements also provide important information because they test our understanding of the relativistic corrections to wave functions and matrix elements.

The first experiment to be sensitive to the relativistic corrections to a two-photon decay rate was a measurement by Marrus *et al.* of the lifetime of the $2\,^1S_0$ state in Kr^{34+} [28]. The only other experiments sensitive to these corrections are measurements of the lifetimes of two-photon emitting states in one- and two-electron nickel [27]. Relativistic corrections have also been tested by studying the $M1$ decay of the $2\,^3S_1$ level in He-like ions [34,35], and single-photon electric dipole ($E1$) decay rates [36–42].

Measurements of the lifetimes of two-photon decays have generally been based on the singles spectrum of photons because of the low count rate for coincidence detection. A limitation in such experiments is the ability to characterize the background under the continuum which could have a complicated dependence on photon energy and decay time. Fluorescence of intense single-photon lines and continuum x-rays from semi-Auger decays [43–45] are examples of processes contributing to this background. Another problem, particularly for the beam-foil excitation used for highly charged ions, is that the one-electron $2\,^2S_{1/2}$ state and the two-electron $2\,^1S_0$ state may both be formed in the experiment. Since they both decay by two-photon emission and have similar lifetimes and end-point energies, it is hard to distinguish between them. These experimental problems were overcome in our earlier measurements in one- and two-electron nickel [27] by using coincidence detection to monitor the decay rate. The requirement of a coincidence with the proper sum energy provides a signature to distinguish background counts and allows separation of one- and two-electron decays. The motivation for the present experiment is to apply the coincidence detection technique to a measurement of the $2\,^1S_0$ lifetime in the higher-Z ion, Br^{33+}, which is more sensitive to relativistic corrections than the Ni^{26+} measurement.

II. EXPERIMENT

This experiment was performed at the ATLAS accelerator at Argonne National Laboratory. The machine provided a 680-MeV beam of $^{79}Br^{21+}$ ions which was further stripped in a 200-$\mu g/cm^2$ carbon foil. The He-like ions made up 20% of the one-particle-nA beam emerging from the foil and the Li-like (+32), Be-like (+31), and B-like (+30) species made up 40%, 25%, and 10%, respectively, of the emerging beam. Ions in the He-like +33 charge state were magnetically selected and directed to the target chamber. The velocity of the beam was measured by a time-of-flight velocity analyzer located between the exit of the linac and the 200-$\mu g/cm^2$ foil. The energy loss in the 200-$\mu g/cm^2$ stripper was determined by a second time-of-flight measurement which compared the arrival times of ions at a fast Faraday cup [46] with and without the 200-$\mu g/cm^2$ stripper foil. The velocity of the beam emerging from the linac was monitored continuously throughout the run, and the energy loss in the stripper foil was measured before, during, and after the experiment. The small energy losses in the target foils (10 and 20 $\mu g/cm^2$) were determined using published energy-loss tables [47,48].

A diagram of the apparatus is given in Fig. 1. A thin foil was moved relative to three fixed Si(Li) detectors which surrounded the beam. The lifetime of the $2\,^1S_0$ level was measured by observing the rate of two-photon coincidences as a function of the foil-detector distance. A shield placed between the foil and the detectors allowed the foil to be brought close to the detectors while preventing them from viewing the beam spot on the foil. The configuration allowed data to be taken with the foil starting 2 mm upbeam of the shield which is a little more than the 1.6 mm decay length of the $2\,^1S_0$ state at our beam velocity. The beam alignment was monitored during the experiment by scanners located before and after

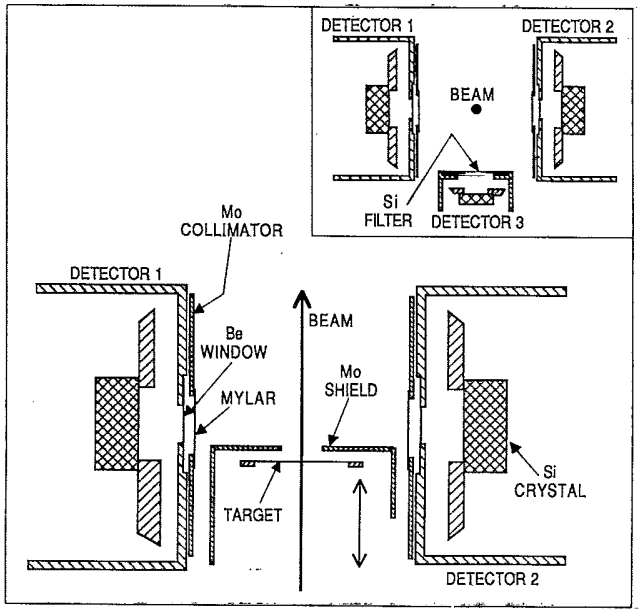

FIG. 1. Experimental arrangement showing the relationship between detectors 1 and 2 and the molybdenum shield. The target is a thin carbon foil which moves (double-ended arrow) relative to the fixed Si(Li) detectors. The inset shows the arrangement of all three Si(Li) detectors. Data on the detectors are given in Table I.

the experimental chamber. The chamber and the scanners were optically aligned with the beam axis before the measurement. The target was translated along the beam axis by a stepping motor controlled by the data-acquisition computer. A linear encoder determined the target position with a resolution of 10 μm. The encoder position was digitized and recorded as part of the data stored for each event.

Properties of the Si(Li) detectors are given in Table I. Detectors 1 and 2 are nearly identical while detector 3 has a thinner, smaller-diameter crystal and a larger-diameter beryllium window. The geometrical arrangement of the detectors was designed to optimize the two-photon coincidence rate while minimizing the sensitivity to changes in the beam size and position. Each detector was calibrated before the experiment using a number of radioactive sources including ^{55}Fe, ^{57}Co, and ^{65}Zn.

A typical spectrum for the Si(Li) detectors is given in Fig. 2. The prominent peak above 10 keV is from single-photon decays of the $n=2$ states of He-like bromine. At short foil detector distances, the triplet and singlet p levels dominate this line but at larger foil-detector distances, it is dominated by the decay of the $2\,^3S_1$ level which has a lifetime of 230 ps [35]. The continuum on the low-energy side of the $M1$ peak comes from individual photons from the two-photon decays. The other prominent features in the spectrum include decays into $n=2$ which contribute x-rays in the region below 4.5 keV and characteristic x rays from fluorescence of the molybdenum shield and collimators.

Three different foils were used, two were 10 μg/cm^2 thick and the other was 20 μg/cm^2 thick. The thinner foils were superior for the measurement because they gave a higher yield for the $2\,^1S_0$ level and a lower yield for most other processes. Data at each target position were taken for a fixed integrated beam current as measured on a Faraday cup located 2 m downbeam of the apparatus. To average over changes in foil or beam properties, 54 individual scans of the decay curve were taken over the course of the measurement. The data were taken in three groups (designated A, B, and C), each of which constituted about $\frac{1}{3}$ of the data reported here.

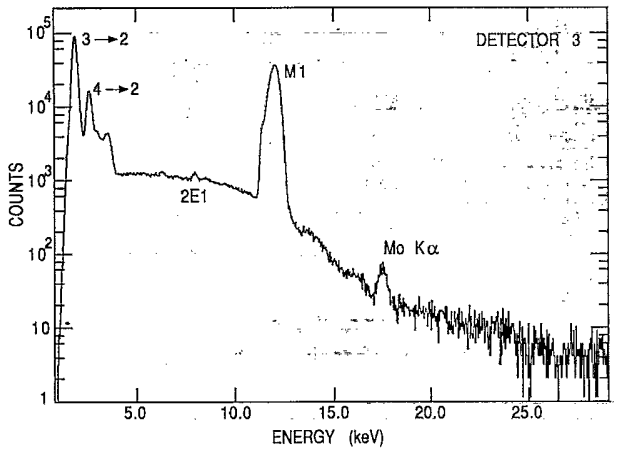

FIG. 2. Typical singles spectrum for detector 3. The energies of the lines are broadened and shifted by the Doppler effect.

TABLE I. Detector geometry and characteristics.

Quantity	Detectors 1 and 2	Detector 3
Detector dimensions (mm)		
Active diameter	9.7	6.2
Sensitive depth	5.33, 5.15	3
Si crystal to Be window	7	3.5
Beam to Be window	15.7	15.5
Be window diam.	4.8	6.5
Molybdenum collim. diam.	8.7	5.0
Absorbing layers (μm)		
Be window	8	8.5
Au layer	0.02	0.02
Inactive Si layer	0.1	0.1
Si filter	NA	6
Mylar	100	NA

Each group used a different foil. For group A which used a 10-μg/cm^2 foil, 3225 two-photon coincidences were recorded at the closest foil position (about 5 coincidences per second) for a collected charge of 11 μC of Br^{33+} ions.

Standard coincidence electronics were used for data collection. The preamplifier outputs for the detectors were sent to both fast and slow amplifiers to give timing and energy signals for each detector. Rise times of 50 ns and 10 μs were used for the fast and slow amplifiers, respectively. Rate-dependent effects such as pileup, dead time, or random coincidences were particular concerns in this experiment. The rates in the detectors were about 1.5 kHz at the smallest foil-detector distance but dropped to a few hundred Hz at the largest distance. Dead time was handled by forcing all detectors and the Faraday cup integrator to have identical dead time. After receiving a fast timing signal from any of the detectors, there was a wait of 1 μs to accept coincidences, and then the fast timing signals, the time-to-amplitude converters, and the Faraday-cup integrator were gated out until the computer and the electronics were ready to process the next event. If two timing signals were received for the same detector within 60 μs, the energy measurement for that detector was considered to be suspect, and that event was tagged as a pileup event. In the data analysis, we rejected pileup events but corrected for the fraction of events rejected at each target position.

Figure 3 is a time-difference spectrum for coincidences between detectors 1 and 2. The prominent peak in the center of the spectrum is mostly true coincidences from two-photon decays of the $2\,^1S_0$ state. Random coincidences that appear to either side exhibit the beam-pulse structure of the linac. The random coincidence rate can be reliably determined by analyzing the events in windows A and B of Fig. 3. These windows are symmetric with respect to the beam-pulse structure. Accidental coincidences between two $M1$ photons are the dominant source of counts in these windows. Such events are not of concern for our experiment because they can be eliminated by placing conditions on the energies of the coincident photons. This point is illustrated by the inset in Fig. 3 which is a portion of the time-difference spectrum with a condition that the individual energies in detectors

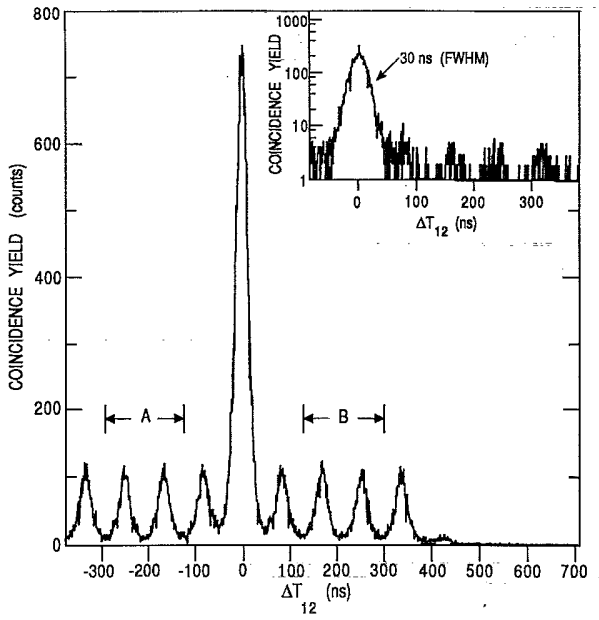

FIG. 3. Time-difference spectrum for coincidences between detector 1 and detector 2. Regions A and B were used for subtraction of randoms. The inset shows the time-difference spectrum with a condition that the individual energies lie within the two-photon continuum (labeled 2E1 in Fig. 2).

1 and 2 lie within the two-photon region (region 2E1 in Fig. 2). With this condition, the rate of random coincidences is greatly reduced compared to the rate of true coincidences. Figure 4 provides a further clarification of the role of random coincidences in the experiment. This shows the correlation between the energies for detectors 1 and 2 for coincident events. The two-photon decays form a diagonal island that satisfies the condition $E_1+E_2=E_0$, where E_0 is the transition energy and E_1 and E_2 are the energies of the individual photons. The

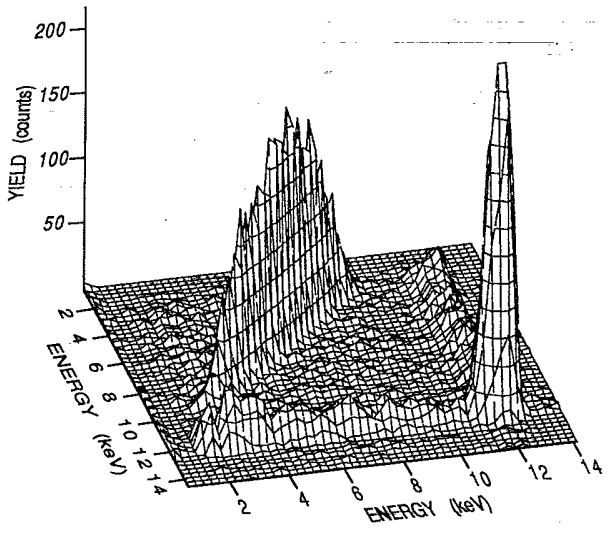

FIG. 4. Correlation of photon energies for coincidences between detector 1 and detector 2. Energies are shifted due to the Doppler effect.

random coincidences are dominated by the events in the peak near 12 keV which are accidental coincidences in which an $M1$ photon is detected by each of the two detectors. Two ridges adjacent to these peaks are accidental coincidences between an $M1$ and a continuum photon. This figure illustrates the good separation between the two-photon decays and the random coincidences.

III. RESULTS

The spectra in Fig. 5 were formed by summing the energies in detectors 1 and 2 for coincidence events. Any event in which a pileup was detected in either detector was rejected. Figure 5(a) includes all events in the prompt peak of the time-difference spectrum (Fig. 3). The peak near 12 keV comes mostly from two-photon decays. The smaller peaks at higher energy are from accidental coincidences. If we require that the individual energies of detectors 1 and 2 lie in the two-photon continua, then most of the accidental coincidences are missing as shown in Fig. 5(b). Figure 5(c) shows the same data but after subtraction of random coincidences as determined by cuts on regions A and B of the time-difference spectrum. This plot illustrates the clean isolation of the two-photon decays. There is a small number of counts on the low-energy side of the two-photon sum-energy peak due to incomplete charge collection in the Si(Li) detectors and escape of silicon K x rays. The silicon escape peak occurs at about 1.8 keV below the full-energy peak. This feature is also observed in our calibration spectra although for the same transition energy it is more prominent in the sum-energy spectra since escape can occur for either photon of the coincidence. Also, the average energy of individual photons contributing to the sum peak is significantly smaller and the probability for escape increases as the energy decreases [49].

The coincidences in Fig. 5(c) are reliably identified as coming from two-photon decays but we also need to distinguish between the H-like and He-like two-photon decays. This distinction can be made based on the fact that

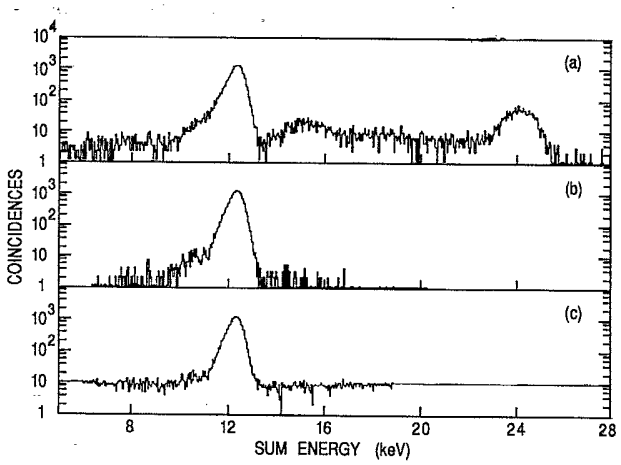

FIG. 5. (a) Sum-energy spectrum for coincidences between detector 1 and detector 2. (b) Sum-energy spectrum with the requirement that the individual energies lie in the two-photon continuum region 2E1 (see Fig. 2). (c) Sum-energy spectrum after subtraction of random coincidences.

the H-like $2\,^2S_{1/2}$ transition energy is 390 eV greater than the transition energy for the He-like $2\,^1S_0$ level. In practice, considerable care is needed in distinguishing these decay modes. Although the intrinsic linewidths in the Si(Li) detectors are about 200 eV at 13 keV, the sum-energy line is considerably broader because each of the photons contributes its intrinsic width and there is significant broadening from the Doppler effect. The line shape and centroid depend in a complicated way on the details of the geometrical arrangement of the detectors and collimators, the beam velocity, beam size, and the angular correlation of the photons. The lifetime of the level is also important because this affects the density of excited ions along the beam axis. We have developed a Monte Carlo simulation program that takes all of these factors into account and predicts the position and shape for each transition line. As a test, the program was first applied to the $M1$ decay of the $2\,^3S_1$ level. Ill-determined parameters (e.g., location of crystals internal to the detectors) were fine tuned to reproduce the shape of the $M1$ line. Using these parameters, we then applied the simulation to the problem of the two-photon decay. Line shapes and positions were calculated for both the H-like and the He-like lines. These calculated shapes were then used to fit our data for the sum-energy spectra for each pair of detectors. The only free parameters in the fits were the intensities of the H-like and He-like components. The most sensitive detector combination was detector 2 and detector 3 since this produced the narrowest sum-energy line. The fit for this coincidence combination is presented in Fig. 6. From this fit we find that $(0.07\pm0.07)\%$ of the total line is due to the H-like component.

There is also a possible contribution from two-photon decay of the $2\,^3S_1$ level in He-like bromine. This level decays to the ground state predominantly by single-photon $M1$ emission but it can also decay by two-photon emission. Calculations for this mode have been done by Drake, Victor, and Dalgarno [20] and by Bely and Faucher [50]. The branching ratio for two-photon decay relative to $M1$ decay in He-like bromine is 5×10^{-4}, and so this process is not expected to affect our experiment. The energy spectrum of individual photons from $2\,^3S_1$ two-photon decays is calculated to be quite different from that of the $2\,^1S_0$ decays in that there is zero transition probability at half the transition energy and broad maxima near either end point. This spectral shape provides an additional suppression for the $2\,^3S_1$ two-photon coincidences in our experiment since our detection efficiency is low in the region of the low-energy maximum.

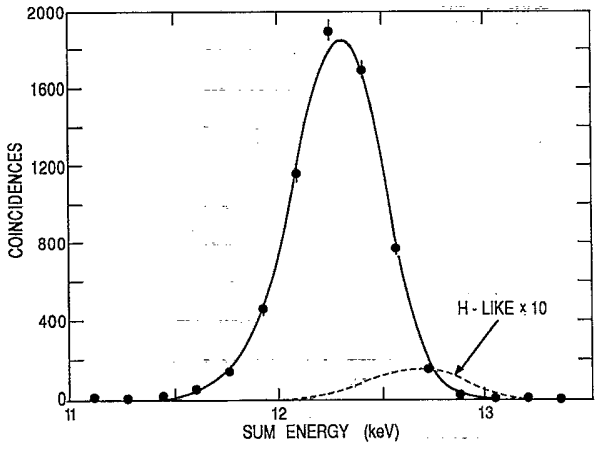

FIG. 6. Sum-energy line for coincidences between detectors 2 and 3 (data points) and a fit (solid line) to the data using line shapes for H-like and He-like two-photon sum-energy lines as determined by the Monte Carlo simulations. The dashed line is 10 times the contribution from H-like decays as determined by the fit.

TABLE II. Results and uncertainties.

Quantity	Lifetime (ps)
Fit result	39.37±0.25
Pileup[a]	(−0.31±0.06)
H-like component[a]	(−0.04±0.04)
Random coincidences[a]	(+0.05±0.01)
Cascades to $2\,^1S_0$	−0.05±0.07
Velocity and position measurement error	±0.11
Beam-movement uncertainty	±0.15
Total	39.32±0.32

[a]The corrections and errors in parentheses are already included in the fit result given in the first line. The fit result includes a correction for time dilation.

We combined the data for each of the three coincidence combinations for each group and corrected for random coincidences, pileup, and H-like component. The resulting decay curves were then fit to a single exponential which determined two parameters: the lifetime and the intensity. The time of flight for each foil position

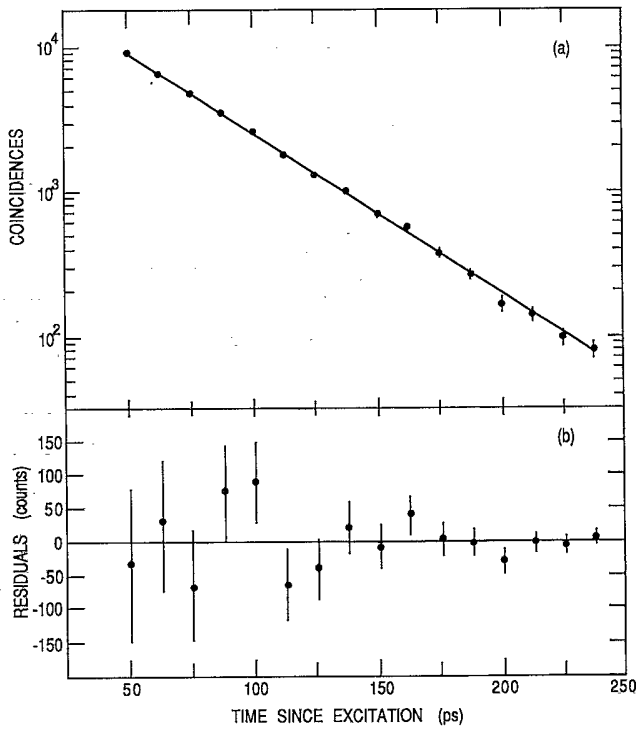

FIG. 7. (a) Decay curve corresponding to all coincidence data, and (b) residuals from a two-parameter fit to the data.

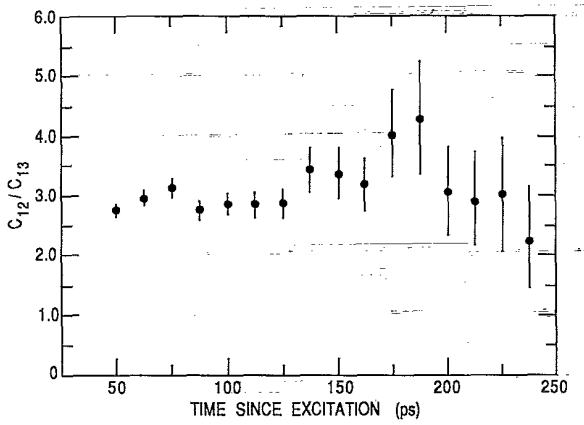

FIG. 8. Ratio between detector 1–detector 2 coincidences C_{12} and detector 1–detector 3 coincidences C_{13} plotted as a function of decay time.

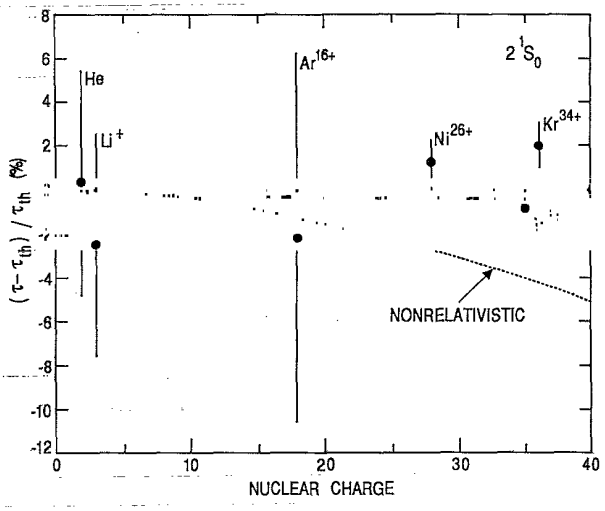

FIG. 9. Comparison of theory and experiment for the lifetime of the $2\,^1S_0$ level in heliumlike ions. The theoretical values τ_{th} are from Drake's calculation, which includes an estimate of relativistic corrections [10]. The differences between experiment and theory are given as a percent of the theoretical values. The error bars refer to the experimental errors, see Ref. [30] (He), Ref [31] (Li^+), Refs. [26,52] (Ar^{16+}), Ref. [27] (Ni^{26+}), this work (Br^{33+}), and Ref. [28] (Kr^{34+}). The theoretical uncertainty is given by the shaded region. The dashed line shows the deviation corresponding to the nonrelativistic theory.

was determined from the measured beam velocity and the average position measured by the position encoder. The results for the three groups agree to within errors so we averaged them to obtain the uncorrected result given in the first row of Table II.

In Fig. 7(a) we show a decay curve together with a two-parameter fit to the data. The residuals for the fit are shown in Fig. 7(b). There is a possible nonrandom "shape" in these residuals that could indicate a systematic error in our experiment. We studied this possibility using the singles data, which provided better counting statistics, but no structures were seen in fits to decay curves formed from the $M1$ line or the two-photon continuum. The only quantities that appear to show a shape as a function of foil position are the ratios of coincidences for different detector combinations. These ratios should be constant as a function of foil position unless there are changes in the beam or the foil that cause a different spatial distribution of ions in the $2\,^1S_0$ level. As illustrated in Fig. 8, there is clearly a nonrandom shape in the ratio of detector 1–detector 2 coincidences to detector-1–detector 3 coincidences. We attribute this shape to incomplete averaging out of changes in the beam or foil during the runs, and we add an additional error to our final result which is designated "beam movement uncertainty" in Table II. We list in Table II the sizes of all errors and corrections that contribute to our final result. Other processes that could contribute systematic errors were considered including collisions with the background gas and Compton scattering, but these processes were found to be negligible.

IV. CONCLUSION

Our final result, $\tau(2\,^1S_0)=39.32(32)$ ps, agrees with Drake's theoretical value of 39.63(16) ps. In Fig. 9 we show a comparison of theory and experiment for all existing data on the lifetime of this level. The present measurement and the measurements in He-like nickel and krypton are the most precise and are also the only results that are sensitive to the relativistic corrections. These results show general agreement between theory and experiment at the level of about 1%.

We can also compare our result to a measurement by Schweppe *et al.* [40] of the decay rate for the $2\,^2P_{1/2}\rightarrow 2\,^2S_{1/2}$ transition in Li-like uranium which has a statistical error of 1.9% and a systematic error of 2.1%. This measurement provides a sensitive test of the relativistic correction to the single-photon $E1$ matrix element for this transition which decreases the decay rate by 37.3%. This measurement is not directly comparable to ours since the calculation of the two-photon decay rate involves a sum over intermediate states and does not factor into a simple matrix element and a phase-space factor. For a crude comparison, we note that the two-photon transition rate depends on the fifth power of the transition energy $\Delta=\omega_i-\omega_f$ [10]. The relativistic corrections increase Δ by 1.4% in Br [51] so the relativistic correction to the factor Δ^5 increases the transition rate by 7.2%. Since the net result of the relativistic corrections is to decrease the rate by 4%, the relativistic correction to the factor containing the dependence on the matrix elements decreases the rate by 11.2%. This is smaller than the relativistic correction for the Li-like uranium matrix element by a factor of 3.3, but the error in our decay rate measurement (0.8%) is smaller by about the same factor, so the two measurements have comparable sensitivity to relativistic corrections.

For the future, it is desirable to improve both the theoretical and experimental results for the decay rate of the $2\,^1S_0$ level to further our understanding of atomic structure in the case where both relativity and electron correlations are important. The study of this decay rate provides information on the atomic wave functions and

matrix elements which complements current efforts to study transition energies in high-Z He-like ions. The relativistic calculations of the lifetime of the $2\,^1S_0$ state are currently only estimates based on one-electron results and are not of high precision. In the case of bromine, for example, the theoretical uncertainty is 0.4%. On the experimental side, the coincidence method appears to have a big advantage in the ability to isolate the two-photon decay mode. The disadvantage of this method is that the count rate is low. However, new injectors and ion sources provide hope for considerably larger beam currents in future experiments. Also, larger arrays of detectors could allow higher coincidence rates while still keeping accidental coincidences and pileup under control. Improved detector resolution would also be desirable since this would allow better isolation of the H-like two-photon decays. The problems of beam movement and changes in the foil composition must also be understood and brought under control. The foil degradation problem might be improved by using a rotating target which would provide better averaging over an uneven foil surface. With these improvements, it is likely that the lifetime of the $2\,^1S_0$ level in Br^{33+} could be measured with an uncertainty of less than 0.2%. This is smaller than the uncertainty in the existing screened hydrogenic theory and so would provide a test for a fully relativistic calculation of the decay rate.

ACKNOWLEDGMENTS

We are indebted to the staff of ATLAS for excellent technical assistance during this experiment. We particularly thank Richard Pardo and John Bogaty, who provided the beam-velocity measurements. This work was supported by the U.S. Department of Energy, Office of Basic Energy Sciences under Contracts No. W-31-109-ENG-38 (ANL), No. DE-FG05-88ER13958 (University of Toledo), and No. DE-FG02-92ER14283 (University of Notre Dame).

[1] M. Goeppert, Naturwissenschaften **17**, 932 (1929).
[2] M. Goeppert-Mayer, Ann. Phys. (Leipzig) **9**, 273 (1931).
[3] G. Breit and E. Teller, Astrophys. J **91**, 215 (1940).
[4] R. Marrus and P. J. Mohr, Adv. At. Mol. Phys. **14**, 181 (1978).
[5] L. Spitzer Jr. and J. L. Greenstein, Astrophys. J. **114**, 407 (1951).
[6] J. Shapiro and G. Breit, Phys. Rev. **113**, 179 (1959).
[7] B. A. Zon and L. I. Rapoport, Pis'ma Zh. Eksp. Teor. Fiz. **7**, 70 (1968); [JETP Lett. **7**, 52 (1968)].
[8] S. Klarsfeld, Phys. Lett. **30A**, 382 (1969).
[9] S. Klarsfeld, Lett. Nuovo Cimento **1**, 682 (1969).
[10] G. W. F. Drake, Phys. Rev. A **34**, 2871 (1986).
[11] W. R. Johnson, Phys. Rev. Lett. **29**, 1123 (1972).
[12] F. A. Parpia and W. R. Johnson, Phys. Rev. A **26**, 1142 (1982).
[13] S. P. Goldman and G. W. F. Drake, Phys. Rev. A **24**, 183 (1981).
[14] S. P. Goldman, Phys. Rev. A **40**, 1185 (1989).
[15] A. Dalgarno, Mon. Not. R. Astron. Soc. **131**, 311 (1966).
[16] A. Dalgarno and G. A. Victor, Proc. Phys. Soc. London **87**, 371 (1966).
[17] G. A. Victor, Proc. Phys. Soc. London **91**, 825 (1967).
[18] G. A. Victor and A. Dalgarno, Phys. Rev. Lett. **18**, 1105 (1967).
[19] V. L. Jacobs, Phys. Rev. A **4**, 939 (1971).
[20] G. W. F. Drake, G. A. Victor, and A. Dalgarno, Phys. Rev. **180**, 25 (1969).
[21] M. Lipeles, R. Novick, and N. Tolk, Phys. Rev. Lett. **15**, 690 (1965).
[22] R. Novick, in *Physics of the One and Two Electron Atoms*, edited by F. Bopp and H. Kleinpoppen (North-Holland, Amsterdam, 1969), p. 296.
[23] M. H. Prior, Phys. Rev Lett. **29**, 611 (1972).
[24] E. A. Hinds, J. E. Clendenin, and R. Novick, Phys. Rev. A **17**, 670 (1978).
[25] C. L. Cocke, B. Curnutte, J. R. MacDonald, J. A. Bednar, and R. Marrus, Phys. Rev. A **9**, 2242 (1974).
[26] R. Marrus and R. W. Schmieder, Phys. Rev. A **5**, 1160 (1972).
[27] R. W. Dunford, M. Hass, E. Bakke, H. G. Berry, C. J. Liu, M. L. A. Raphaelian, and L. J. Curtis, Phys. Rev. Lett. **62**, 2809 (1989).
[28] R. Marrus, V. S. Vicente, P. Charles, J. P. Briand, F. Bosch, D. Liesen, and I. Varga, Phys. Rev. Lett. **56**, 1683 (1986).
[29] A. S. Pearl, Phys. Rev. Lett. **24**, 703 (1970).
[30] R. S. Van Dyck, Jr., C. E. Johnson, and H. A. Shugart, Phys. Rev. A **4**, 1327 (1971).
[31] M. H. Prior and H. A. Shugart, Phys. Rev. Lett. **27**, 902 (1971).
[32] W. R. Johnson and J. Sapirstein, Phys. Rev. A **46**, 2197 (1992).
[33] H. G. Berry, R. W. Dunford, and A. E. Livingston, Phys. Rev. A **47**, 698 (1993).
[34] R. Marrus, P. Charles, P. Indelicato, L. de Billy, C. Tazi, J. Briand, A. Simionovici, D. D. Dietrich, F. Bosch, and D. Liesen, Phys. Rev. A **39**, 3725 (1989).
[35] R. W. Dunford, D. A. Church, C. J. Liu, H. G. Berry, M. L. A. Raphaelian, M. Hass, and L. J. Curtis, Phys. Rev. A **41**, 4109 (1990).
[36] C. T. Munger and H. Gould, Phys. Rev. Lett. **57**, 2927 (1986).
[37] R. Hutton, L. Engström, and E. Träbert, Phys. Rev. Lett. **60**, 2469 (1988); see also C. Guet, S. A. Blundell, and W. R. Johnson, Phys. Lett. A **143**, (1990).
[38] R. Marrus, A. Simionovici, P. Indelicato, D. D. Dietrich, P. Charles, J.-P. Briand, K. Finlayson, R. Bosch, D. Liesen, and F. Parente, Phys. Rev. Lett. **63**, 502 (1989).
[39] I. Martinson, Nucl. Instrum. Methods Phys. Res., Sect. B **43**, 323 (1989).
[40] J. Schweppe, A. Belkacem, L. Blumenfeld, N. Claytor, B. Feinberg, H. Gould, V. E. Kostroun, L. Levy, S. Misawa, J. R. Mowat, and M. H. Prior, Phys. Rev. Lett. **66**, 1434 (1991).
[41] P. Indelicato, B. B. Birkett, J.-P. Briand, P. Charles, D. D. Dietrich, R. Marrus, and A. Simionovici, Phys. Rev. Lett. **68**, 1307 (1992).
[42] C. E. Tanner, A. E. Livingston, R. J. Rafac, F. G. Serpa, K. W. Kukla, H. G. Berry, L. Young, and C. A. Kurtz, Phys. Rev. Lett. **69**, 2765 (1992).
[43] T. Åberg and J. Utrianen, Phys. Rev. Lett. **22**, 1346 (1969).

[44] T. Åberg, in *Atomic Inner-shell Processes,* edited by B. Crasemann (Academic, New York, 1975), p. 353.
[45] E. M. Bernstein, C. Kozhuharov, P. H. Mokler, T. Stöhlker, J. Ullrich, and Z. Stachura, in *GSI Scientific Report 1991,* edited by U. Grundinger (GSI, Darmstadt, Federal Republic of Germany, 1992).
[46] J. M. Bogaty, R. C. Pardo, and B. E. Clift (unpublished).
[47] J. F. Ziegler, *Handbook of Stopping Cross Sections for Energetic Ions in All Elements* (Pergamon, New York, 1980).
[48] F. Hubert, R. Bimbot, and H. Gauvin, At. Data Nucl. Data Tables **46**, 1 (1990).
[49] D. D. Cohen, Nucl. Instrum. Methods **178**, 481 (1980).
[50] O. Bely and P. Faucher, Astron. Astrophys. **1**, 37 (1969).
[51] G. W. F. Drake, Can. J. Phys. **66**, 586 (1988).
[52] H. Gould and R. Marrus, Phys. Rev. A **28**, 2001 (1983).